4 *Tempering of Bainite*

4.1 Introduction

Tempering is a term historically associated with the heat treatment of martensite in steels. It describes how the microstructure and mechanical properties change as the metastable sample is held isothermally at a temperature where austenite cannot form. The changes during the tempering of martensite can be categorised into stages. During the first stage, excess carbon in solid solution segregates to defects or forms clusters within the solid solution. It then precipitates, either as cementite in low-carbon steels, or as transition iron-carbides in high-carbon alloys. The carbon concentration that remains in solid solution may be quite large if the precipitate is a transition carbide. Further annealing leads to stage 2, in which almost all of the excess carbon is precipitated, and the carbides all convert into more stable cementite. Any retained austenite may decompose during this stage. Continued tempering then leads to the spheroidisation of carbides, extensive recovery of the dislocation structure, and finally to the recrystallisation of the ferrite plates into equiaxed grains.

The description presented above is idealised. Many of the reactions ascribed to stage 1 can occur *during* the formation of the martensite when the martensite-start temperature is high, a phenomenon known as *autotempering*. Bainite forms at even higher temperatures so autotempering becomes an unavoidable part of the transformation. The redistribution of carbon from supersaturated ferrite into the residual austenite, and the precipitation of carbides during the bainite reaction, occur rapidly and are genuine autotempering effects (Fig. 4.1). The purpose of this Chapter is to deal primarily with the tempering effects which occur when a bainitic microstructure is reheated; the *in situ* tempering phenomena are described elsewhere in the text.

The rate of change of the microstructure and properties during tempering is expected to scale with the degree to which the virgin sample deviates from equilibrium. Bearing this in mind, there are a number of essential differences between the tempering behaviour of bainite and that of martensite.

Bainitic ferrite contains little carbon in solid solution since much of it is precipitated as cementite particles which are coarse when compared with tempered martensitic microstructures. Secondary hardening reactions in alloy

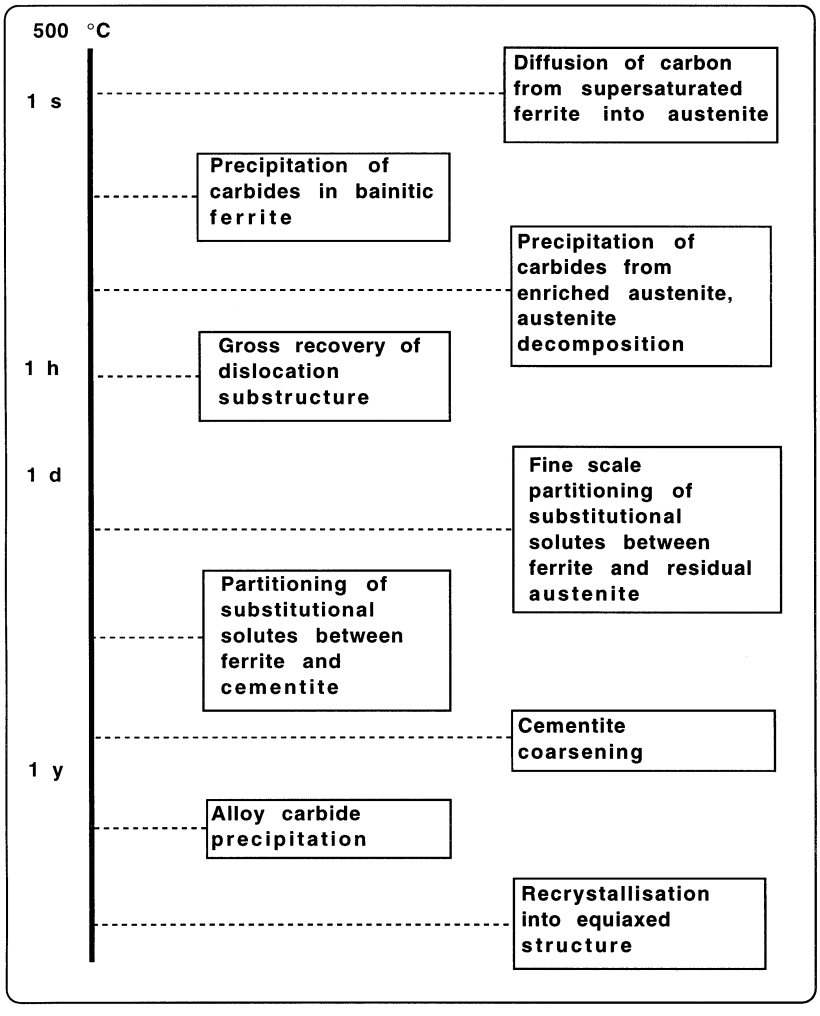

Fig. 4.1 The time scales associated with a variety of tempering phenomena for bainite.

steels with a bainitic microstructure are slower than with martensite, because the coarser cementite particles take longer to dissolve (Woodhead and Quarell, 1965). Secondary hardening involves the replacement of metastable cementite with substitutional-solute-rich alloy carbides.

When compared with martensite, bainite grows at relatively high temperatures where the microstructure undergoes recovery during transformation. The extent of this recovery is larger than would be associated with autotempered martensite. Consequently, when low-carbon steel bainitic microstructures are

annealed at temperatures as high as 700 °C (1 h), there is only a slight increase in recovery, and little change in the morphology of the ferrite platelets or the number density of the carbide particles (Irvine *et al*., 1957; Bush and Kelly, 1971).

Rapid softening occurs only when the plates of ferrite change into equiaxed ferrite. Whether this change is due simply to grain growth or to recrystallisation has not been investigated. In the former case it is the excess surface energy which constitutes the driving force, whereas during recrystallisation, it is the stored energy due to defects such as dislocations or due to elastic strains in the lattice which provides the major component of the driving force for the reaction. During the change to a more equiaxed microstructure, the cementite spherodises and coarsens considerably. Continued tempering then causes much smaller changes in hardness with time.

In marked contrast with martensitic steels, small variations in the carbon concentration (0.06–0.14 wt%) have little effect on the bainite tempering curve (Fig. 4.2). Carbon has a potent solid solution strengthening effect. Thus, the strength of martensite drops sharply as the carbon precipitates during tempering. For bainitic microstructures, the carbon is not in solid solution but is

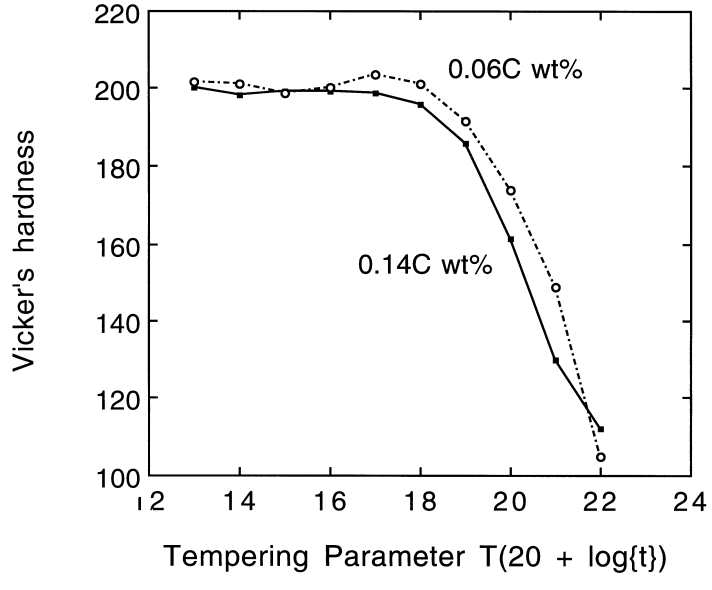

Fig. 4.2 Change in hardness for two bainitic steels containing different carbon concentrations, as a function of a time–temperature tempering parameter (after Irvine and Pickering, 1957). The tempering parameter is defined with the absolute temperature T and the time t in hours.

precipitated as coarse carbides which contribute little to strength (Irvine and Pickering, 1957; Irvine *et al*., 1957). It is expected therefore that the tempering response of bainite is insensitive to the average carbon concentration.

4.2 Tempering Kinetics

It is astonishing that there is as yet no quantitative model for the kinetics of tempering, certainly not of the kind that could be used in the design of alloys or heat-treatments. Figure 4.2 illustrates an empirical method of expressing tempering data using a time–temperature parameter, useful because it permits interpolation between experimental data and a method of estimating the effect of anisothermal heat treatments which are common in industrial practice.

The method has its origins in some pioneering work by Holloman and Jaffe (1945), who proposed that the effectiveness of an isothermal heat treatment should be related to the product:

$$t \exp\{-Q/RT\} \tag{4.1}$$

where Q is an effective activation energy and the other terms have their usual meanings. The product is the integral of the curve of $\exp\{-Q/RT\}$ versus time. To estimate the period required to achieve the same metallurgical effect at another temperature simply involves the assumption that the product $t \exp\{-Q/RT\}$, once evaluated, is constant irrespective of temperature. The product is often called the *kinetic strength* of the heat treatment and provides a rough method for combining the influence of time and temperature. The concept is difficult to justify, especially in circumstances where the driving force varies with temperature or where the mechanism of the metallurgical process alters with temperature. The parameter and many related parameters have nevertheless been useful in cases where rigorous solutions do not exist. Examples include the representation of creep data, weld microstructure calculations (Alberry *et al*., 1977, 1979, 1983; Ashby *et al*., 1982, 1984, 1987), and the rationalisation of martensite tempering data (Hollomon and Jaffe, 1945). Irvine and Pickering have demonstrated its usefulness in representing the hardness of tempered bainite.

4.3 Tempering of Steels Containing Austenite

The decomposition of retained austenite during the heat treatment of martensite in quenched steels occurs during the second stage of the tempering process. Appreciable quantities of retained austenite are usually only present in quenched steels which have carbon concentrations in excess of about 0.4 wt%. The conventional wisdom is that the austenite decomposes to bainite but it has

[12:16 3/9/01 C:/3B2 Templates/keith/3750 BAINITE.605/3750-004.3d] Ref: 0000 Auth: Title: Chapter 00 Page: 94 91-116

been demonstrated that the decomposition occurs by instead a reconstructive mechanism (Kennon and Burgess, 1978).

In many bainitic steels, the alloy composition is chosen to avoid the retention of austenite. However, large quantities of austenite can be retained in silicon-rich bainitic steels, in two forms: as thin films between the ferrite plates and as blocks between different sheaves of bainite. Both are enriched in carbon but the films more so because of their isolation between plates of ferrite.

4.3.1 Redistribution of Substitutional Solutes

There is no partitioning of substitutional solutes during the bainite reaction, in spite of the requirements of equilibrium. Given the opportunity, they should tend to redistribute in a manner which leads to a reduction in the overall free

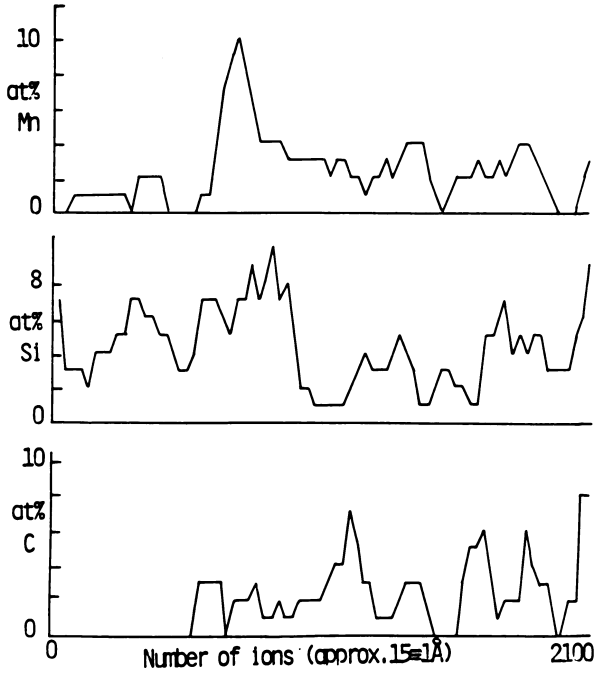

Fig. 4.3 A field ion microscope/atom-probe experiment on an alloy Fe–0.43C–2.24Si–2.82Mn wt%, heat treated at 328 °C for 11 days. This produces a mixture of bainitic ferrite and austenite with the reaction stopping after the first few minutes at temperature, the subsequent holding simply leading to an annealing of the microstructure. The diagram illustrates the composition profile obtained across the austenite/bainitic ferrite interface, which is identified by the point where significant levels of carbon begin to be detected. (Stark *et al*., 1990).

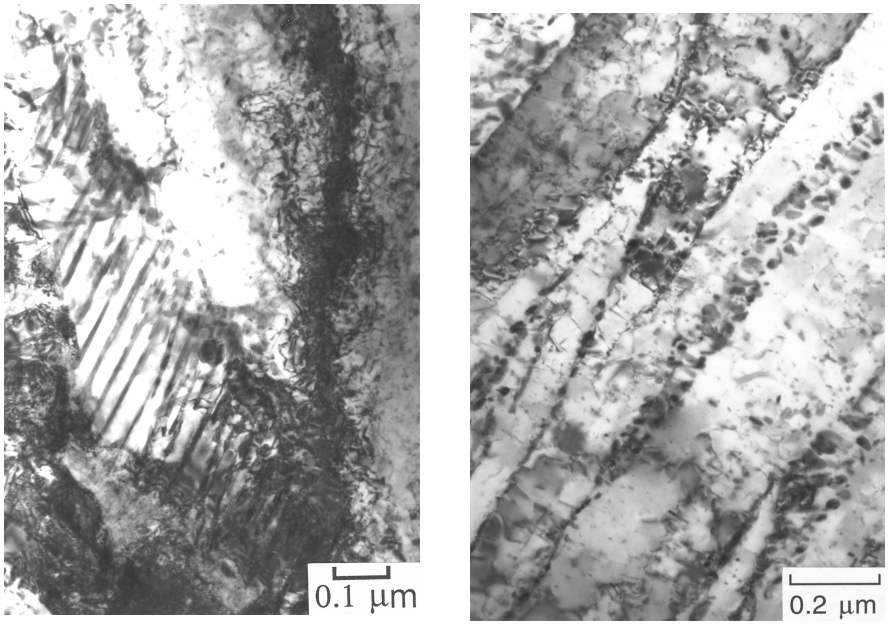

Fig. 4.4 Transmission electron micrographs illustrating the effect of tempering a mixture of bainitic ferrite and retained austenite, in a Fe–3Mn–2Si–0.4C wt% alloy, at 500 °C for 60 min. The austenite is supersaturated with respect to carbides. (a) The larger blocks of austenite tend to decompose into pearlite. (b) Arrays of discrete carbide particles form between the sub-units of bainitic ferrite when the films of austenite decompose. The microstructure prior to tempering consisted of just bainitic ferrite and residual carbon-enriched austenite.

energy. It is found that when a mixture of bainitic ferrite and austenite is tempered at low temperatures, the solutes partition before the austenite begins to decompose. The partitioning is on a fine scale and can only be detected using atomic resolution techniques. Figure 4.3 illustrates one such experiment, in which a mixture of bainitic ferrite and austenite was annealed at 328 °C for 11 days. There is clear evidence for the diffusion of manganese into the austenite at the interface, with a corresponding depletion zone in the adjacent ferrite.

4.3.2 Decomposition of Austenite

When the carbon concentration in all the regions of untransformed austenite is larger than or equal to that given by the T_0' curve, tempering can only induce further transformation by a mechanism involving the diffusion of carbon. The austenite may decompose into a mixture of ferrite and carbides if its carbon

concentration exceeds that given by the extrapolated $\gamma/(\gamma +$ carbide) phase boundary (Fig. 3.1b). The larger regions of austenite form colonies of pearlite with a fine interlamellar spacing, whereas the films of austenite decompose into discrete particles of cementite in a matrix of ferrite (Figure 4.4). The films are too thin to permit the onset of the cooperative growth needed to establish a pearlite colony. The T_c (Fig. 3.1b) condition for carbide formation may not be satisfied when tempering at high temperatures, in which case the austenite can transform to ferrite although, not by a bainitic mechanism.

Tempering need not involve a separate heat-treatment. Microstructural changes can occur when austenite is transformed isothermally to bainite, and then held at the transformation temperature for longer than is necessary to complete the bainite reaction. For example, any residual austenite may decompose slowly as the microstructure attempts to approach equilibrium. There is less bainite and more residual austenite at higher transformation temperatures; this combined with the greater atomic mobility at high temperatures leads to the formation of pearlite colonies following the bainite reaction. Bhadeshia and Edmonds (1979a) reported a case where transformation at a temperature close to B_S led to the formation of upper bainite within a matter of minutes, to be followed some 30 h later by pearlite. Figure 4.5 illustrates, in

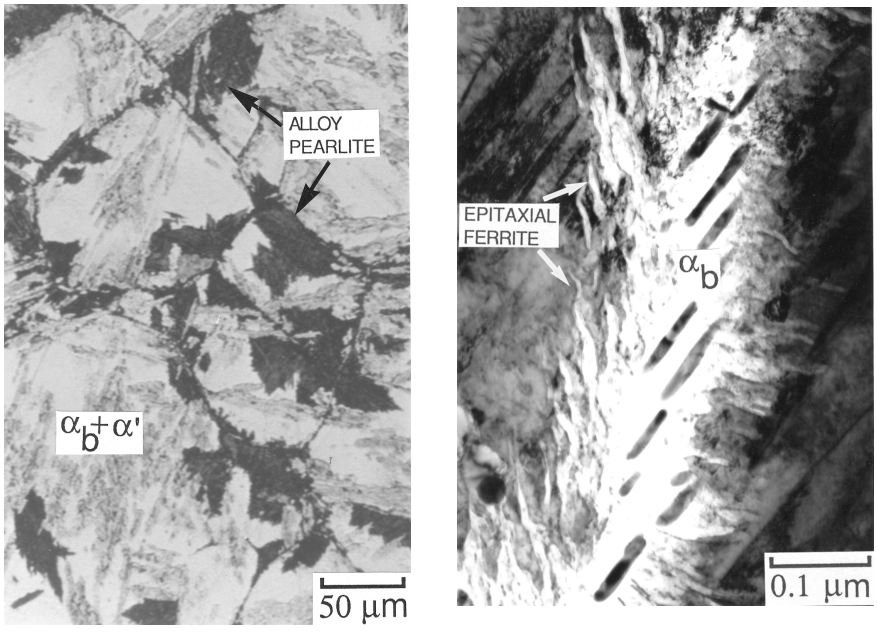

Fig. 4.5 The decomposition of residual austenite once the bainite reaction has stopped. (a) Pearlite colonies; (b) ferrite growing epitaxially from bainite plates.

another alloy, two different reconstructive reactions occurring after the bainite stopped following 30 min at temperature. Continued holding at the isothermal transformation temperature for 43 days led to the decomposition of residual austenite at an incredibly slow rate into two different products (Bhadeshia, 1981b, 1982b). The first of these is alloy pearlite which nucleates at the austenite grain boundaries and develops as a separate transformation. In the other, the original bainite/austenite interfaces move to produce epitaxial growth by a reconstructive mechanism (Fig. 4.5). The interfaces degenerate into a series of irregular perturbations. The ferrite in the perturbations has the same crystallographic orientation as the original bainite – it is in fact contiguous with the bainitic ferrite. It grows with the same substitutional solute content as the parent austenite but does not cause an IPS shape change. It is incredible that the perturbations took 43 days to grow to a length comparable to the thickness of the original bainite plates, which completed transformation in a matter of seconds. Reconstructive growth is bound to be much slower than displacive transformation at low homologous temperatures.

4.4 Coarsening of Cementite

Coarsening leads to a minimisation of the energy that is stored in a sample in the form of interfaces. The rate equation for a coarsening process controlled by the diffusion of solute through the matrix is given by (Greenwood, 1956; Lifshitz and Slyozov, 1961; Wagner, 1961):

$$\overline{r}^3 - \overline{r}_o^3 = (8\sigma^{\theta\alpha} c^{\alpha\theta} D_{eff} V_m^{\theta} t)/9RT \tag{4.2}$$

where V_m^{θ} is the molar volume of cementite, $c^{\alpha\theta}$ is the concentration of carbon in ferrite which is in equilibrium with cementite, $\overline{r}_3$ is the mean particle radius at time t and $\overline{r}_o^3$ is the mean particle radius at time zero, the moment when coarsening is defined to begin. $\sigma^{\theta\alpha}$ is the cementite–ferrite interface energy per unit area ($\simeq 690\,\mathrm{J\,m^2}$, Li *et al*., 1966) and D_{eff} is an effective diffusion coefficient for carbon in ferrite. Since there is little change in precipitate volume fraction during coarsening, the diffusion of carbon is coupled to that of iron in such a way that the total volume remains constant. D_{eff} is then given by (Li *et al*., 1966):

$$D_{eff} = \frac{n_{Fe} D_{Fe}^{\alpha} D_C^{\alpha} \Omega_{Fe} [\Omega_{Fe} + (n_C/n_{Fe})\Omega_C]}{(n_{Fe} D_{Fe}^{\alpha} \Omega_{Fe}^2) + (n_C D_C^{\alpha} \Omega_C^2)} \tag{4.3}$$

where n_{Fe} and n_C are the numbers of iron or carbon atoms per unit volume of ferrite respectively, D_{Fe}^{α} and D_C^{α} are the respective diffusivities of iron and carbon in ferrite, Ω_{Fe} is the volume per atom of ferrite and Ω_C is the volume of a molecule of Fe_3C less $3\Omega_{Fe}$. It has been shown that equation 4.3 describes to a fair accuracy, the coarsening kinetics of cementite during the tempering of

both upper and lower bainite in a Fe–0.67C–0.73Mn–0.27Si wt% commercial steel (Deep and Williams, 1975). The agreement with theory is best for the higher tempering temperatures, with an underestimation of the coarsening rate at lower temperatures. This discrepancy has been attributed to grain boundary diffusion contributing more to the net flux at low temperatures.

In fact, the microstructures of both tempered martensite and bainite contain two kinds of cementite particles, those located at the lath boundaries and a finer distribution within the laths. In upper bainite the cementite is located only at the lath boundaries. Figure 4.6 shows experimental data on the coarsening of cementite during the tempering of a medium carbon steel. The upper bound of each shaded region represents the lath-boundary cementite, the lower bound the intra-lath cementite. The bainitic microstructure is coarse to begin with because of the tempering inherent in the formation of bainite. With martensite the tempering induces the precipitation of cementite, with considerable intra–lath cementite and a larger overall number density of particles. Therefore, the coarsening rate is much larger for martensite; the bainitic microstructure shows greater stability to tempering. A consequence is that the matrix microstructure remains fine over a longer time period for bainite than for martensite.

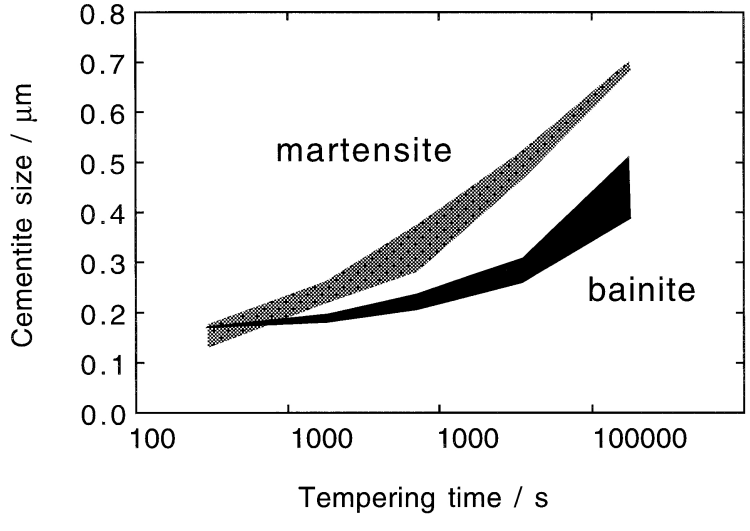

Fig. 4.6 Changes in the size of cementite particles as a function of the tempering time at 700 °C, with different starting microstructures. The upper bound of each shaded region represents the mean size of particles located at lath boundaries. The lower bound corresponds to particles within the laths. The data are for a Fe–0.45C–0.22Si–0.62Mn wt% steel; the bainite was produced by isothermal transformation at 380 °C. After Nam (1999).

A model which deals with the coarsening of cementite under conditions where both grain boundary and lattice diffusion are important has been presented by Venugopalan and Kirkaldy (1977). It takes account of the simultaneous coarsening of carbide particles and ferrite grains, allows for the multicomponent nature of alloys steels and works remarkably well in predicting the mean particle size, ferrite grain size and strength of tempered martensite; it has yet to be applied to bainite.

Elementary coarsening theory suggests that the time-independent particle size distribution, normalised relative to the mean particle radius, should be skewed towards large particles, with a sharp cut off at a normalised radius of 1.5. However, measured distributions for cementite in bainite do not fit this behaviour, the distributions instead being skewed towards smaller particle sizes. Deep and Williams point out that this behaviour is also found for cementite in tempered martensite.

4.5 Secondary Hardening and the Precipitation of Alloy Carbides

Secondary hardening is usually identified with the tempering of martensite in steels containing strong carbide forming elements like Cr, V, Mo and Nb. The formation of these alloy carbides necessitates the long-range diffusion of substitutional atoms and their precipitation is consequently sluggish. Carbides like cementite therefore have a kinetic advantage even though they may be metastable. Tempering at first causes a decrease in hardness as cementite precipitates at the expense of carbon in solid solution, but the hardness begins to increase again as the alloy carbides form. Hence the term *secondary hardening*. Coarsening eventually causes a decrease in hardness at long tempering times so that the net hardness versus time curve shows a secondary hardening peak.

There is no reason to suspect that the secondary hardening of bainite should be particularly different from that of martensite. Early work did not reveal any pronounced peaks in the tempering curves for bainite, perhaps because of the low molybdenum concentration in the steels used (Irvine *et al*., 1957). The peaks were subsequently found during the tempering of a vanadium containing bainitic steel but not for Cr or Mo containing bainitic steels (Fig. 4.7, Irvine and Pickering, 1957). An unexplained observation was that for the Mo containing steels, the carbide formed on tempering bainite is initially cementite, which then transforms to $(Fe, Mo)_{23}C_6$, whereas on tempering martensite in the same steels the ultimate carbides are found to be Mo_2C

Later work revealed clear evidence of secondary hardening in low carbon bainitic steels containing up to 2.95 wt% Mo, 2.12 wt% Cr and also in vanadium containing bainitic steels (Baker and Nutting, 1959; Irvine and Pickering,

[12:16 3/9/01 C:/3B2 Templates/keith/3750 BAINITE.605/3750-004.3d] Ref: 0000 Auth: Title: Chapter 00 Page: 100 91-116

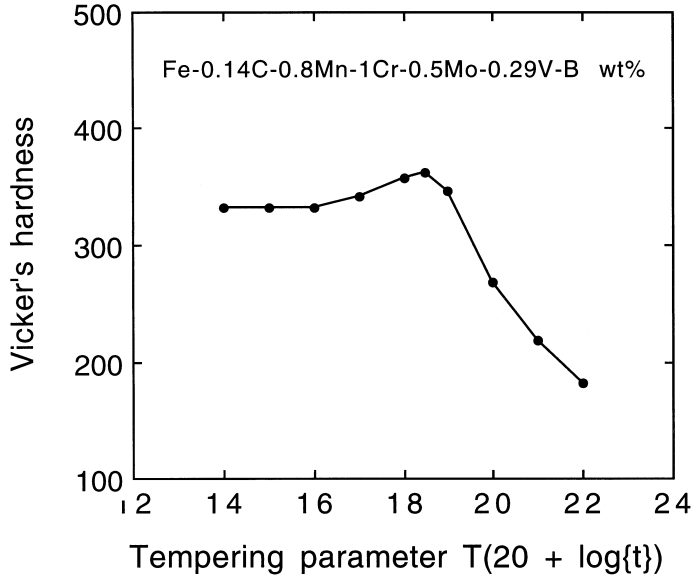

Fig. 4.7 Secondary hardening peak in a vanadium-containing bainitic steel (after Irvine and Pickering, 1957). The tempering parameter is defined with the absolute temperature T and the time t in hours.

1957). Whether or not *peaks* are observed in the tempering curves, the data are all consistent with secondary hardening because the tempering resistance is improved relative to plain carbon steels.

It would be interesting to see whether it is possible to design a steel in which the bainite secondary hardens as it forms. The B_S temperature would have to be around 650 °C and the alloy would have to be engineered to avoid interference from other transformation products.

4.6 Changes in the Composition of Cementite

The cementite that precipitates from austenite during the course of the bainite reaction has the same substitutional to iron atom ratio as the austenite, i.e. there is no partitioning of the substitutional solutes. Its composition is therefore far from equilibrium. Tempering helps the cementite to approach its equilibrium composition by the diffusion of solutes from the ferrite into the cementite.

Most of the chemical data on cementite composition changes during tempering have been obtained using either direct chemical analysis of extracted carbides, or energy dispersive X-ray analysis techniques associated with transmission electron microscopy. These techniques are not well suited for the analysis of carbon or nitrogen concentrations. These two elements can

mix to form carbonitrides. Thus, atom-probe field ion microscopy has shown that M_2C carbides found in tempered bainite have an average composition $[Cr_{0.41}Mo_{0.59}]_2[C_{0.96}N_{0.04}]$ (Josefsson *et al.*, 1987; Josefsson, 1989). In the discussion that follows, we shall neglect to consider the carbon and nitrogen, for which there are few data.

Some of the first results on the tempering of bainite were obtained by Baker and Nutting (1959) for a commercial steel with a chemical composition Fe–0.15C–2.12Cr–0.94Mo wt%. The cementite was found to become richer in Cr, Mo and Mn, the degree of enrichment being highest for Cr, with its concentration eventually reaching some 20 wt% (Fig. 4.8).

The enrichment of cementite decreases as alloy carbide formation begins, until the cementite eventually starts to dissolve (Fig. 4.9). This is expected since a dissolving particle of cementite will contain a chromium depleted zone in the cementite near the moving ferrite/austenite interface.

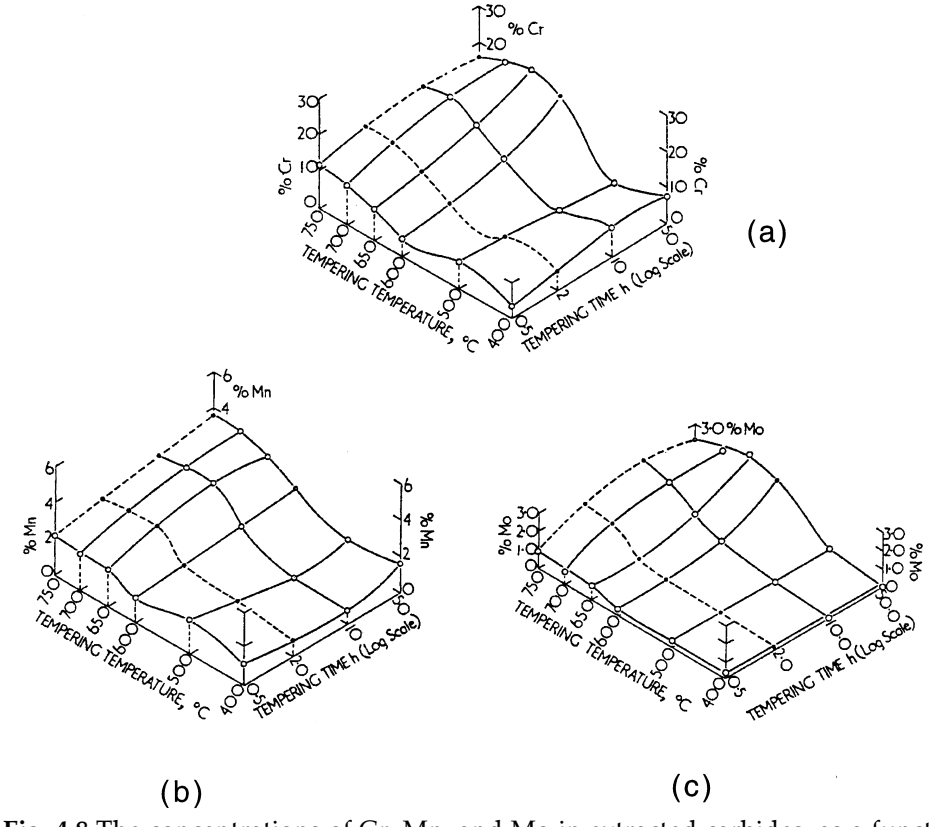

Fig. 4.8 The concentrations of Cr, Mn, and Mo in extracted carbides, as a function of the tempering time and temperature, for a steel with initial microstructure which is bainite (Baker and Nutting, 1959).

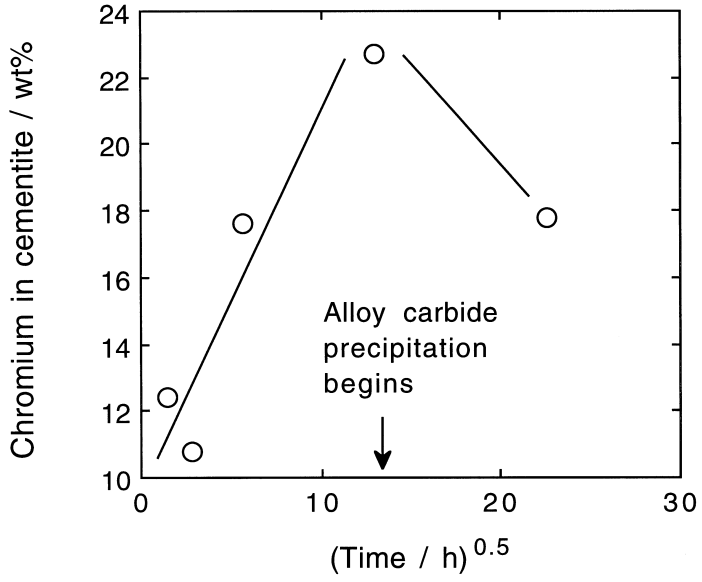

Fig. 4.9 Mean chromium concentration in cementite found in a tempered bainitic microstructure aged at 565 °C, in a '$2\frac{1}{4}$Cr1Mo' power plant steel (Thomson, 1990).

4.6.1 Remanent Life Prediction

The study of changes in the chemical composition of carbides during the tempering of bainite is of commercial importance. Where creep resistant bainitic steels are in service at elevated temperatures over long time periods (30 years), it is important for safety reasons to know accurately the time–temperature history of the steel at any stage during service. The thermal history of the steel can be related to the amount of creep life remaining in that steel, before the accumulated damage becomes intolerable. This remaining creep life is in the power generation industry called the *remanent life* (Bhadeshia *et al.*, 1998).

The accurate estimation of remanent life permits the safe use of existing power plant beyond their original design lives. The method can also help anticipate plant closures or it can facilitate the timely replacement of components. Power plant temperatures fluctuate and are difficult to record over long periods of time and for the large number of components involved (Fig. 4.10). Life assessment therefore has to be made on a conservative basis, which leads to expense due to premature closure of plant which has not exhausted its safe life. Any method which gives an accurate measure of the thermal history experienced by the steel during service can lead to savings by enabling more accurate assessments of the remaining creep life. At first sight, the obvious

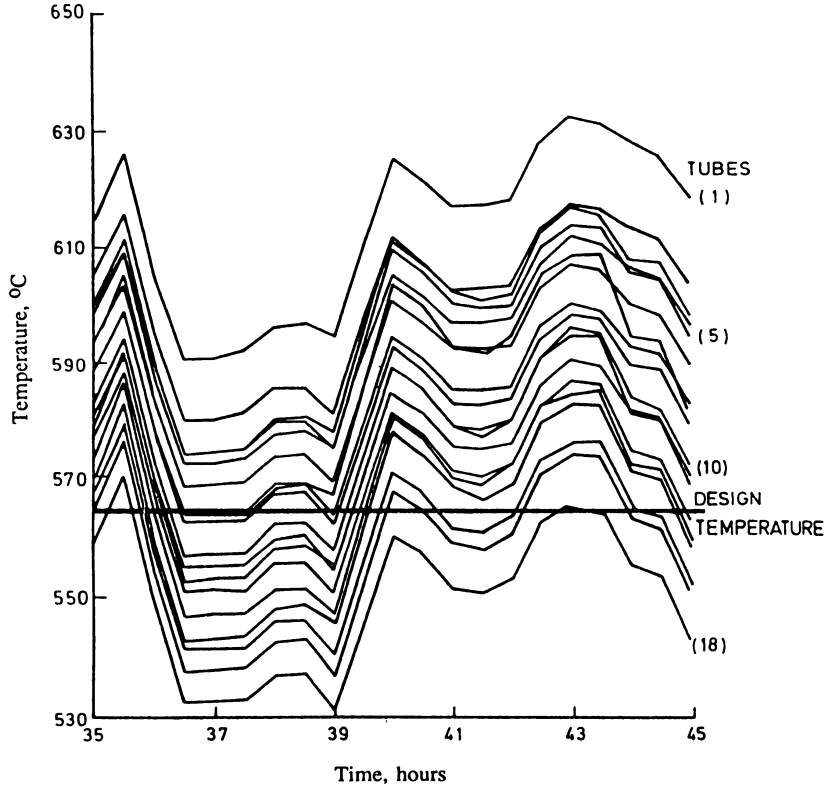

Fig. 4.10 Illustration of the variation in the temperature at different locations on a particular component ('reheater drum') of a 500 MW power station (Cane and Townsend, 1984).

thing to do would be to monitor the temperature everywhere using strategically located thermocouples, but this is impractical over the large time span involved and in the harsh environment of the power station.

The microstructure of the steel, and especially the chemical composition of the cementite, changes during service. These changes can be exploited to assess the effective thermal history experienced by the steel since its implementation. The microstructure is in this context, a recorder of time and temperature; for example, the cementite particles in the steel can be monitored by removing a few using extraction replicas. Their compositions can then be measured using a microanalysis technique to determine the extent of enrichment and hence an estimate of the effective service temperature. The interpretation and extrapolation of such data relies on the existence of theory capable of relating the

[12:16 3/9/01 C:/3B2 Templates/keith/3750 BAINITE.605/3750-004.3d] Ref: 0000 Auth: Title: Chapter 00 Page: 104 91-116

cementite composition to heat treatment. Such theory is discussed in a later section, after an introduction to the published work.

The use of cementite composition for thermal history assessment was first applied to the cementite in pearlite, where it was found empirically that the Cr and Mn concentrations varied with $t^{\frac{1}{3}}$, where t is the time at tempering temperature (Carruthers and Collins, 1981). We shall see later that a $t^{\frac{1}{2}}$ relationship can be justified theoretically.

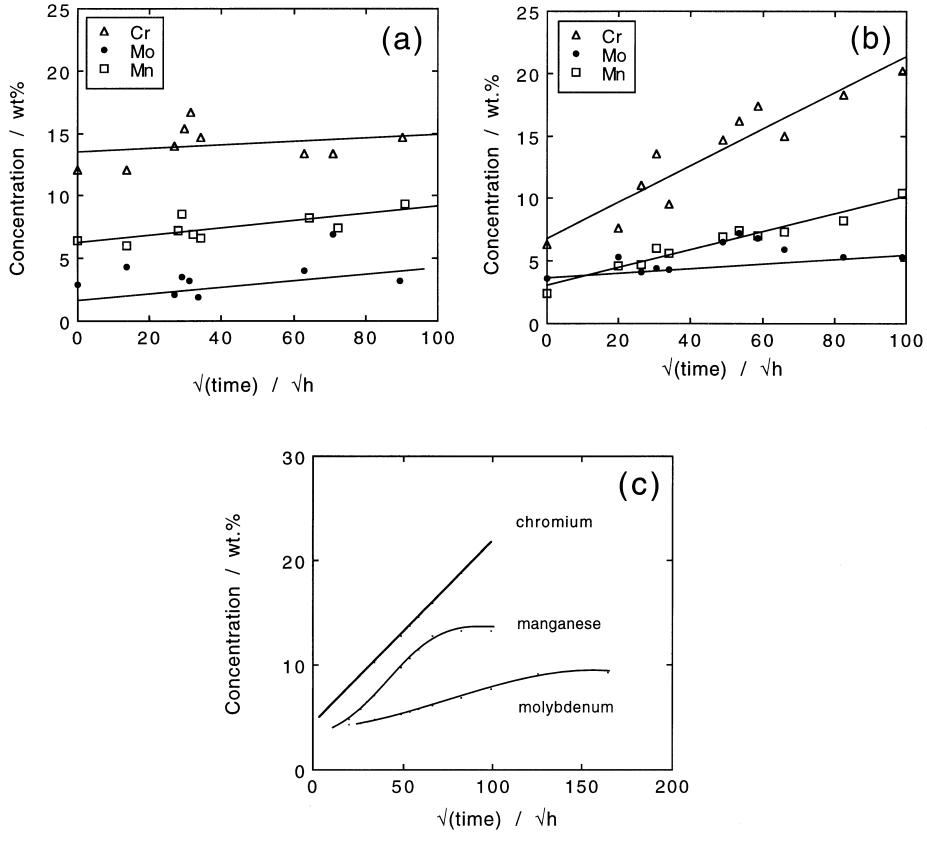

Fig. 4.11 Measured changes in the chemical composition of cementite particles as a function of the square root of time, during ageing at 550 °C. The steel composition is Fe–0.1C–0.24Si–0.48Mn–0.84Cr–0.48Mo wt%. The data have been replotted against $t^{\frac{1}{2}}$ instead of $t^{\frac{1}{3}}$ used in the original work. (a) Tempered at 550 °C following service at 565 °C for 70000 h. (b) Heat treated to give a fully bainitic microstructure, stress-relieved at 693 °C for one hour and then tempered at 550 °C for the periods illustrated. Data from Afrouz *et al*. (1983). (c) Finite difference calculations showing that the enrichment process will inevitably show deviations from the parabolic law at long ageing times (Bhadeshia, 1989).

Afrouz *et al*. (1983) reported similar results on a bainitic steel. The alloy was normalised to give a microstructure of allotriomorphic ferrite and 20% bainite, was then tempered in an unspecified way, and held at 565 °C for 70000 h at a stress of ≃17 MPa. This service-exposed material was then examined after further tempering at 550 °C for a range of time periods. As expected, the chromium and manganese concentrations of the cementite (M_3C) increased with time, the manganese possibly showing signs of saturation during the later stages of ageing, and the data for molybdenum exhibiting considerable scatter (Fig. 4.11).

Afrouz *et al*. also austenitised the service-exposed material so that after oil-quenching, a fresh fully bainitic microstructure was obtained; it is likely that both upper and lower bainite were present. This was then tempered at 693 °C for an hour to give coarse M_3C particles at the lath boundaries and within the bainite, and subsequently held at 550 °C for a variety of time periods. The change in M_3C composition was monitored during the latter tempering treatment (Fig. 4.11). The starting composition of the carbide is of course leaner than that of the service-exposed material and the rate of enrichment was found to be higher for the reheat-treated samples (Fig. 4.11).

4.6.2 *Theory for Carbide Enrichment*

The process by which carbide particles enrich during tempering has been analysed theoretically (Bhadeshia, 1989). The method is similar to the one employed in determining the time required to decarburise supersaturated plates of ferrite, as discussed in detail in Chapter 6. The kinetics of cementite composition change are given by:

$$t_c^{\frac{1}{2}} = \frac{c^{\theta}(\overline{c}_X - c_X)\pi^{\frac{1}{2}}}{4D^{\frac{1}{2}}(c_X^{\alpha\theta} - \overline{c}_X)} \tag{4.4}$$

where t_c is the time required for the carbide to reach a concentration c_X (the subscript represents a substitutional solute), and c_θ is the thickness of the cementite plate (Fig. 4.12a). D is the diffusion coefficient for the solute in the matrix (assumed to be identical to the corresponding diffusivity in the particle) and $c_X^{\alpha\theta}$ is the concentration of the substitutional solute in the ferrite which is in equilibrium with the cementite. A further outcome is that the carbide composition should depend on its size (Fig. 4.12b).

The time dependence of concentration is found to be $t^{\frac{1}{2}}$ rather than the $t^{\frac{1}{3}}$ which has been assumed in the past. The analysis neglects the overlap of the diffusion fields of different particles, an effect which is inevitable during long term heat treatment. This can be tackled using finite difference methods, which show that the time exponent must vary with time, since the boundary condi-

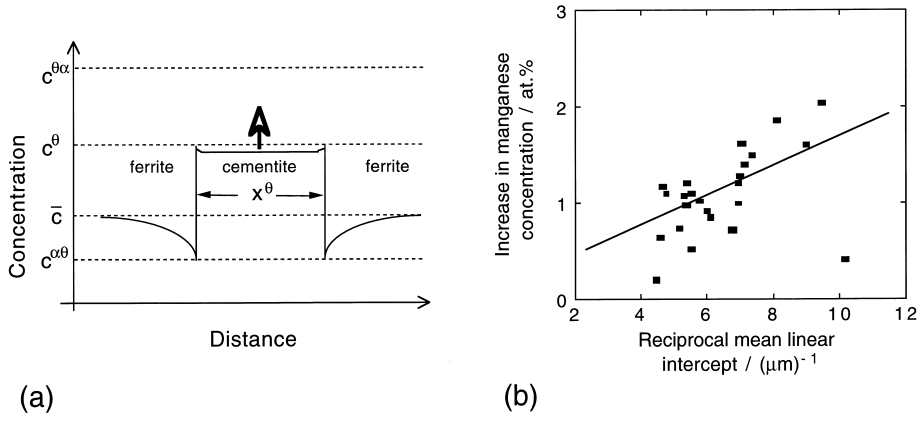

Fig. 4.12 (a) Solute concentration profile that develops during enrichment of cementite. $c^{\theta\alpha}$ is the concentration in cementite which is in equilibrium with ferrite. (b) Size dependence of the cementite chemical composition, for particles extracted from a bainitic microstructure aged for 4 weeks at 565 °C (Wilson, 1991). Detailed analysis shows that the scatter in the data is a consequence of the micro-analysis technique.

tions for the diffusion process change with the onset of soft impingement (Fig. 4.11c).

4.6.3 Effect of Carbon on Carbide Enrichment

There are two effects which depend on the carbon concentration of the steel. The ternary Fe–Cr–C phase diagram on the M_3C/α field shows that an increase in the carbon concentration is accompanied by a decrease in the equilibrium concentration of chromium in the carbide. Thus, the carbide enrichment rate is expected to decrease. A further effect is that the volume fraction of cementite increases, in general leading to an increase in particle thickness and volume fraction. The thickness increase retards the rate of enrichment (equation 4.4). If the carbide particles are closer to each other then soft-impingement occurs at an earlier stage, giving a slower enrichment at the later stages of annealing.

Local variations in carbon concentration may have a similar effect as changes in average concentration. Such variations can be present through solidification induced segregation, or because of microstructure variations caused by differences in cooling rates in thick sections. It is well known that the microstructure near the component surface can be fully bainitic with the core containing a

[12:16 3/9/01 C:/3B2 Templates/keith/3750 BAINITE.605/3750-004.3d] Ref: 0000 Auth: Title: Chapter 00 Page: 107 91-116

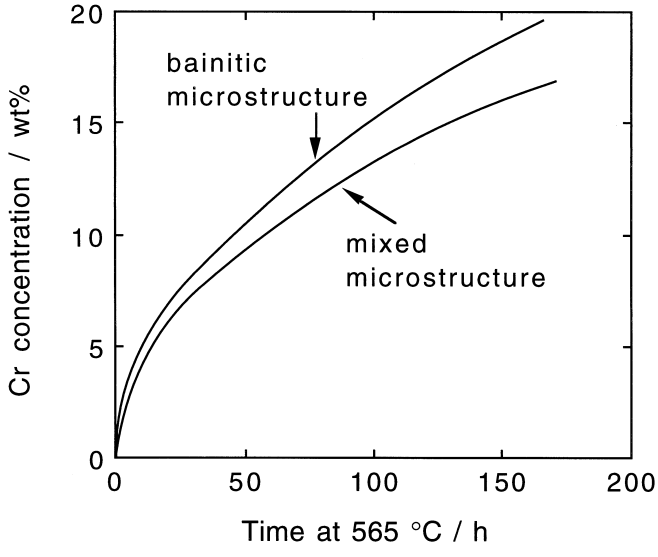

Fig. 4.13 $2\frac{1}{4}$Cr1Mo steel, cementite enrichment in a fully bainitic microstructure and one which is a mixture of allotriomorphic ferrite and bainite (Thomson and Bhadeshia, 1994).

large amount of allotriomorphic ferrite in addition to bainite. In the latter case, the bainite which grows after the allotriomorphic ferrite, transforms from high carbon austenite. The associated carbides are then found to enrich at a slower rate (Fig. 4.13). This discussion emphasises the role of carbon.

4.7 Sequence of Alloy Carbide Precipitation

Cementite is not the equilibrium carbide in many bainitic alloy steels, but it is nevertheless kinetically favoured because its growth mechanism does not require the long-range diffusion of substitutional solutes. The equilibrium combination of phases naturally depends on the steel composition. Alloy carbides become vital in steels where the resistance to creep deformation is of paramount importance; they obviously play a role in secondary hardened steels for use at ambient temperatures but such alloys tend to be martensitic rather than bainitic. Figure 4.14 shows the equilibrium phases to be found in creep-resistant steels. $M_{23}C_6$, M_2X and small fractions of carbonitrides are the equilibrium precipitates in the first two alloys which are generally used in the bainitic or partly bainitic microstructures. The other higher alloy steels are martensitic and are susceptible to the formation of Laves phases (intermetallic compounds). It is interesting that cementite is not an equilibrium phase in any of the alloys illustrated.

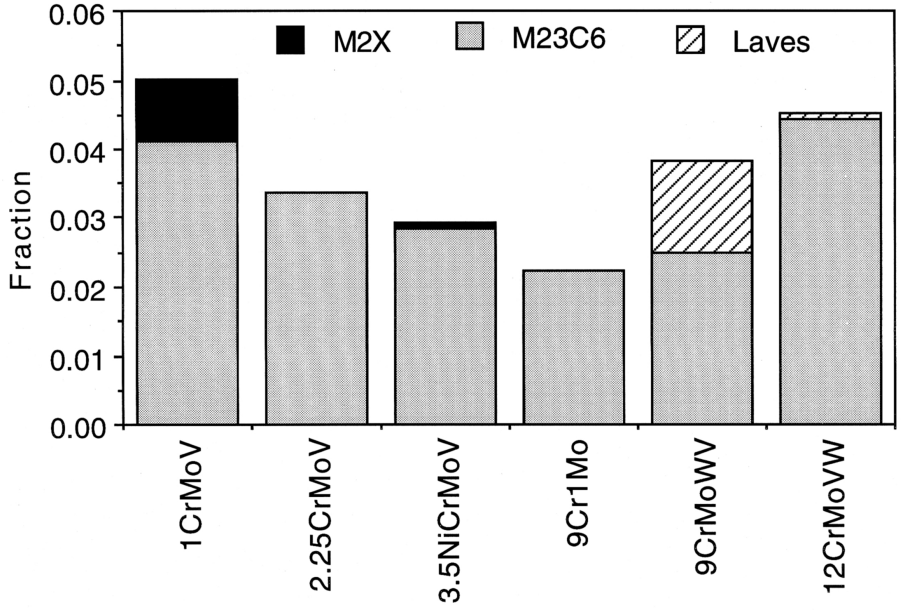

Fig. 4.14 Equilibrium fractions of carbides at 565 °C (838 K) in some common power plant steels, the first two of which frequently are bainitic. The remaining alloys are essentially martensitic. The detailed chemical compositions are given in Table 12.2. Small fractions of vanadium and niobium carbonitrides are present in some steels but are not shown. Thus, the modified 9Cr1Mo contains 0.0009 NbN and 0.003 VN, the 9CrMoWV steel contains 0.0008 NbN and 0.0032 VN.

The approach to equilibrium can be slow, especially when the tempering temperature is less than 600 °C. The change from cementite to the equilibrium carbide may occur via a number of other transition carbides. Baker and Nutting (1959) showed that during the tempering of bainite Fe–2.12Cr–0.94Mo–0.15C wt%, the first alloy carbide to form is M_2C, needles of which precipitate independently of the cementite (Fig. 4.15). Later work has shown that the M_2C contains substantial amounts of other elements; it is better represented as M_2C (Woodhead and Quarrel, 1965; Murphy and Branch, 1971). This applies to virtually all the alloy carbides in multicomponent steels.

M_7C_3 starts to form soon after the precipitation of M_2C, perhaps at the interface between the Cr-enriched cementite and ferrite. M_2C then begins to dissolve, giving way to $M_{23}C_6$. Both $M_{23}C_6$ and M_7C_3 are at high temperatures, completely or partly replaced by the equilibrium carbide M_6C.

With the exception of M_2C, new transition carbides seem to precipitate in association with preexisting carbides. The sequence of changes in Fe–2.12Cr–0.94Mo–0.15C wt% can be summarised as follows:

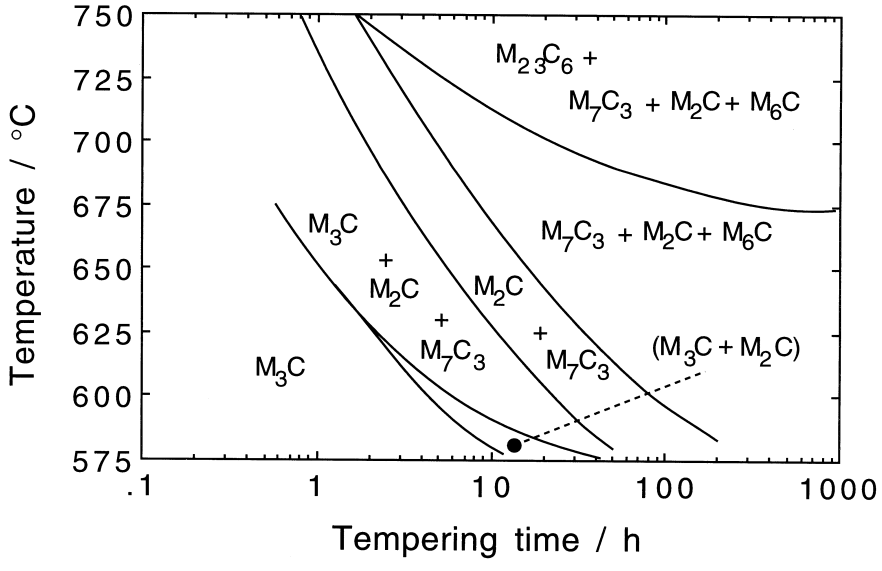

Fig. 4.15 An updated version of the classic Baker–Nutting carbide stability diagram for a $2\frac{1}{4}$Cr1Mo steel (after Nutting, 1998).

$$\begin{array}{l} \theta \rightarrow \theta + \mathrm{M_2C} \rightarrow \mathrm{M_{23}C_6} \rightarrow \mathrm{M_6C} \\ \quad\downarrow \\ \mathrm{M_7C_3} \rightarrow \qquad\quad \rightarrow \mathrm{M_6C} \end{array} \tag{4.5}$$

A different sequence has been reported by Pilling and Ridley (1982) for lower carbon Fe–Cr–Mo–C alloys containing lower carbon concentrations (0.018–0.09 wt%) which illustrates the sensitivity of the microstructure to the precise chemical composition:

$$\begin{array}{l} \theta \rightarrow \mathrm{M_2C} \rightarrow \mathrm{M_{23}C_6} \rightarrow \mathrm{M_6C} \\ \quad + \\ \mathrm{M_7C_3} \rightarrow \qquad\quad \rightarrow \mathrm{M_7C_3} \end{array} \tag{4.6}$$

Yu (1989) has shown that an increase in the silicon concentration to about 0.6 wt% stabilises (M_6C which is absent in silicon-free $2\frac{1}{4}$Cr1Mo steels) since silicon has a relatively high solubility in that carbide. It was also found to accelerate the precipitation of M_2C. An increase in the manganese concentration from 0 to 0.8 wt% was found to accelerate M_7C_3 precipitation. Enhanced chromium concentrations are known to accelerate the formation of $M_{23}C_6$ and

Table 4.1 Concentration (in wt%) of the major alloying elements in the steels used to demonstrate the model.

	C	N	Mn	Cr	Mo	Ni	V	Nb
$2\frac{1}{2}$Cr1Mo	0.15	–	0.50	2.12	0.9	0.17	–	–
3Cr1.5Mo	0.1	–	1.0	3.0	1.5	0.1	0.1	–
10CrMoV	0.11	0.056	0.50	10.22	1.42	0.55	0.20	0.50

this influences the sensitivity of the microstructure to severe hydrogen attack (Ritchie *et al.*, 1984; Spencer *et al.*, 1989).

Some of these detailed kinetic effects of the average composition of the steel on the precipitation processes can now be predicted theoretically (Robson and Bhadeshia, 1997). The compositions of three steels used for illustration are given in Table 4.1. These three alloys, whilst of quite different chemical compositions, show similar precipitation *sequences* but on vastly different time scales. For example, at 600 °C the time taken before $M_{23}C_6$ is observed is 1 h in the 10CrMoV steel, 10 h in the 3Cr1.5Mo alloy and in excess of 1000 h in the $2\frac{1}{4}$Cr1Mo steel.

A plot showing the predicted variation of volume fraction of each precipitate as a function of time at 600 °C is shown in Fig. 4.16. Consistent with experiments, the precipitation kinetics of $M_{23}C_6$ are predicted to be much slower in the $2\frac{1}{4}$Cr1Mo steel compared to the 10CrMoV and 3Cr1.5Mo alloys. One contributing factor is that in the $2\frac{1}{4}$Cr1Mo steel a relatively large volume fraction of M_2X and M_7C_3 form prior to $M_{23}C_6$. These deplete the matrix and therefore suppress $M_{23}C_6$ precipitation. The volume fraction of M_2X which forms in the 10CrMoV steel is relatively small, and there remains a considerable excess of solute in the matrix, allowing $M_{23}C_6$ to precipitate rapidly. Similarly, in the 3Cr1.5Mo steel the volume fractions of M_2X and M_7C_3 are insufficient to suppress $M_{23}C_6$ precipitation to the same extent as in the $2\frac{1}{4}$Cr1Mo steel.

Phase equilibrium is, of course, a function of temperature as well as the chemical composition. Precipitation sequences may therefore change with the temperature. In a Fe–1Cr–1Mo–0.75V–(B, Ti) wt% bainitic steel Collins (1989) showed that tempering led to the formation of TiC and V_4C_3, both of which also contained molybdenum. The V_4C_3 nucleates on TiC particles which form first. The TiC then converts *in situ* into molybdenum-rich M_2C precipitates. At 600 °C the stability of the carbides is in the following sequence

$$M_2C > V_4C_3 > TiC$$

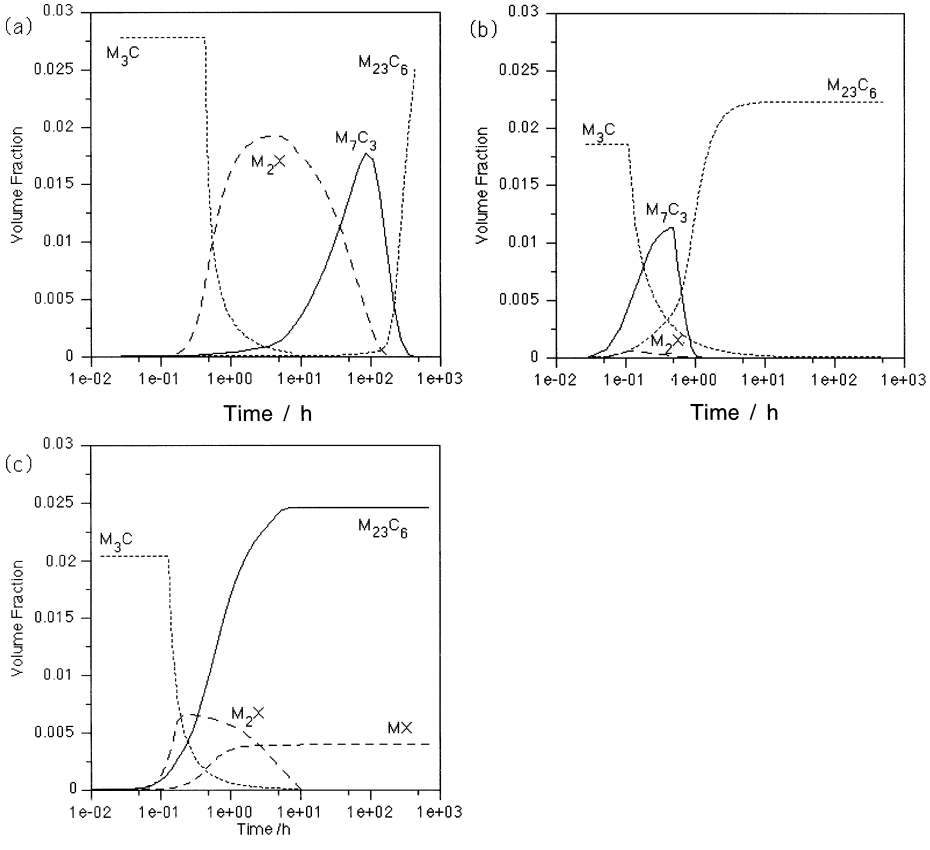

Fig. 4.16 The predicted evolution of precipitate volume fractions at 600 °C for three power plant materials (a) $2\frac{1}{4}$Cr1Mo (b) 3Cr1.5Mo and (c) 10CrMoV.

whereas at higher temperatures, the V_4C_3 is more stable than M_2C. The dependence on temperature is important because creep tests are often accelerated by raising the test temperature but the carbide structure at the higher temperature may be different, making the accelerated test unrepresentative.

4.7.1. Effect of Starting Microstructure on Tempering Reactions

There are no major differences in the alloy carbide precipitation reactions when the microstructure is changed from martensite to bainite (Baker and Nutting, 1959). If allotriomorphic ferrite is present in the microstructure then it may already contain alloy carbides which precipitate during the diffusional growth of the ferrite itself. In the $2\frac{1}{4}$Cr1Mo steel M_2C precipitates present in the ferrite

[12:16 3/9/01 C:/3B2 Templates/keith/3750 BAINITE.605/3750-004.3d] Ref: 0000 Auth: Title: Chapter 00 Page: 112 91-116

dissolve during tempering to be replaced by M_6C particles. By contrast, alloy carbides do not form during the growth of any of the displacive transformation products, including bainite and martensite.

The distribution and type of precipitates is also influenced by the microstructure (Lee, 1989). Thus, M_2C forms the main precipitate within a tempered bainite plate whereas mixtures of cementite, M_2C, M_7C_3 and $M_{23}C_6$ are found at the bainite plate boundaries. The boundaries are not only more effective heterogeneous nucleation sites but the cementite particles located there are sources of carbon for the precipitation of alloy carbides.

Any differences in the number density or distribution of nucleation sites will cause changes in the kinetics of precipitation reactions. The equilibrium carbide M_6C forms more rapidly in bainite than in pearlite or allotriomorphic ferrite (Lee, 1989).

4.8 Changes in the Composition of Alloy Carbides

Alloy carbides cannot form without the long-range diffusion of substitutional solutes. Given this *necessary* diffusion, it is not surprising that their compositions are at all times close to equilibrium. Small changes can be induced by one or more of the following phenomena:

1. The equilibrium chemical composition of particles with curved interfaces is dependent on the radius of curvature via the Gibbs–Thompson effect.
2. The phase rule allows greater degrees of freedom in steels containing one or more substitutional solutes. Thus, the tie-line controlling the equilibrium composition of the carbide may shift during the precipitation reaction, either as the solute content of the matrix is depleted or as other phases precipitate (Fujita and Bhadeshia, 1999).
3. Carbides adjust to a new equilibrium when the tempering temperature is changed (Strang *et al.*, 1999). It is common in industrial practice to use multiple tempering heat-treatments.

4.9 Precipitation Hardening with Copper

Unlike carbides or oxides, copper is regarded as a soft precipitate in iron; it strengthens the iron by about 40 MPa per wt% but does not cause a decrease in toughness.

Copper-bearing low-carbon steels with a mixed microstructure of ferrite and pearlite are used in heavy engineering applications which demand a combination of strength, toughness and weldability. These low carbon steels transform to carbide-free bainite, with thin films of retained austenite between the bainite

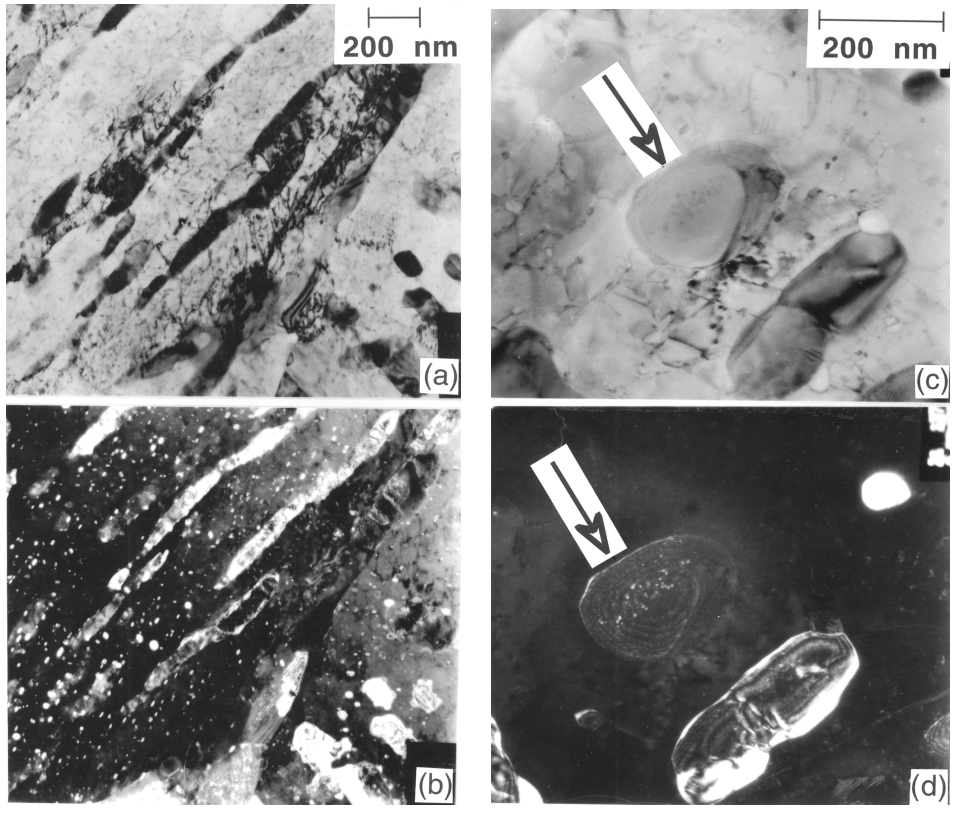

Fig. 4.17 Copper precipitation in bainite obtained by isothermal transformation at 350 °C for 65 minutes, followed by tempering at 550 °C for many hours (Fourlaris *et al.*, 1996). (a,b) Bright field transmission electron micrograph and corresponding dark field image showing copper precipitation in tempered bainitic ferrite. (c,d) Bright field and corresponding dark field image of copper precipitates in the cementite associated with bainite.

plates (Thompson *et al.*, 1988). Fine particles of copper in the bainitic ferrite contribute to the overall strength.

The precipitation of copper occurs from supersaturated bainite as a consequence either of autotempering or when the steel is deliberately tempered (Fourlaris *et al.*, 1996). Thus, no precipitation could be detected following the transformation of some experimental Cu-rich steels in the range 200–400 °C, either in the bainitic ferrite or in its associated cementite. Subsequent tempering at 550 °C resulted in fine copper precipitates in both the ferrite and cementite phases (Fig. 4.17). Copper, which is a substitutional solute, is not in this respect different from any secondary hardening element in steels.

[12:16 3/9/01 C:/3B2 Templates/keith/3750 BAINITE.605/3750-004.3d] Ref: 0000 Auth: Title: Chapter 00 Page: 114 91-116

A potential difficulty in quenched and tempered copper precipitation strengthened steels is their tendency to crack during stress-relief heat treatments following welding (Wilson *et al.*, 1988). Although the steels are immune to cold cracking, the copper particles are taken into solution in the heat-affected zone during welding. The stress-relief heat treatment then causes precipitation which hinders the annealing of residual stresses.

4.10 Summary

There are important differences in the tempering behaviour of bainite and martensite, because the former autotempers during transformation. Much of the carbon precipitates or partitions from the ferrite during the bainite reaction. Since $B_S > M_S$, the extent of autotempering is greatest for bainite, which consequently is less sensitive to additional tempering heat-treatments. The decrease in strength on tempering bainite is smaller because unlike martensite, there is hardly any carbon in solid solution. Major changes in strength occur only when the microstructure coarsens or with the onset of recrystallisation where equiaxed grains of ferrite replace the bainite plates. Minor changes in strength are due to cementite particle coarsening and a general recovery of the dislocation substructure. Bainitic steels containing strong carbide forming elements show secondary hardening similar to martensitic steels. In most cases, new carbides nucleate on existing metastable carbides, with the exception of M_2C which forms in isolation on dislocations.